The Proteomic Profile of Circulating Pentraxin 3 (PTX3) Complex in Sepsis Demonstrates the Interaction with Azurocidin 1 and Other Components of Neutrophil Extracellular Traps*[S]

Kenji Daigo‡, Naotaka Yamaguchi§, Takeshi Kawamura‡, Koichi Matsubara¶, Shuying Jiang¶‖, Riuko Ohashi¶, Yukio Sudou‖, Tatsuhiko Kodama, Makoto Naito¶, Kenji Inoue‡‡, and Takao Hamakubo‡§§**

Pentraxin 3 (PTX3), a long pentraxin subfamily member in the pentraxin family, plays an important role in innate immunity as a soluble pattern recognition receptor. Plasma PTX3 is elevated in sepsis (~200 ng/ml) and correlates with mortality. The roles of PTX3 in sepsis, however, are not well understood. To investigate the ligands of PTX3 in sepsis, we performed a targeted proteomic study of circulating PTX3 complexes using magnetic bead-based immunopurification and shotgun proteomics for label-free relative quantitation via spectral counting. From septic patient fluids, we successfully identified 104 candidate proteins, including the known PTX3-interacting proteins involved in complement activation, pathogen opsonization, inflammation regulation, and extracellular matrix deposition. Notably, the proteomic profile additionally showed that PTX3 formed a complex with some of the components of neutrophil extracellular traps. Subsequent biochemical analyses revealed a direct interaction of bactericidal proteins azurocidin 1 (AZU1) and myeloperoxidase with PTX3. AZU1 exhibited high affinity binding (K_D = 22 ± 7.6 nM) to full-length PTX3 in a calcium ion-dependent manner and bound specifically to an oligomer of the PTX3 N-terminal domain. Immunohistochemistry with a specific monoclonal antibody generated against AZU1 revealed a partial co-localization of AZU1 with PTX3 in neutrophil extracellular traps. The association of circulating PTX3 with components of the neutrophil extracellular traps in sepsis suggests a role for PTX3 in host defense and as a potential diagnostic target. ***Molecular & Cellular Proteomics 11: 10.1074/mcp.M111.015073, 1–12, 2012.***

Pentraxin 3 (PTX3)[1] is a secretory protein classified as a long pentraxin subfamily member of the pentraxin family. The pentraxin family proteins, which are evolutionarily conserved multimeric pattern recognition receptors and share a pentraxin-like domain in the C terminus, are recognized as key components of humoral innate immunity (1). PTX3 has a unique 200-amino acid domain in its N terminus and is known to play multiple roles, including the regulation of inflammatory reactions, innate resistance to pathogens, and female fertility (2). PTX3 is expressed in a variety of cells at inflammatory sites (3) and is also stored in neutrophil-specific granules (4). The stored PTX3 in neutrophils is released into the extracellular space and localizes to neutrophil extracellular traps (NETs) (4), which are extracellular fibers consisting of DNA, histones, and antimicrobial proteins that capture and kill pathogens (5). PTX3 is useful as a diagnostic marker of vascular damage and infections (6). In septic patients, the circulating PTX3 concentration increases to an especially high level (7).

Sepsis is one of the major causes of death in developed countries (8). Despite extensive studies, an effective treatment is not yet available. During the past few decades, sepsis has come to be recognized as a heterogeneous, complex, and dynamic syndrome caused by imbalances in the inflammatory network (9). It has been accepted that sepsis develops through two stages: an initial pro-inflammatory response, de-

From the ‡Department of Molecular Biology and Medicine and the **Laboratory for Systems Biology and Medicine, Research Center for Advanced Science and Technology, The University of Tokyo, Tokyo 153-8904, Japan, the Departments of §Emergency and Critical Care Medicine and ‡‡Cardiology, Juntendo University Nerima Hospital, Tokyo 177-0033, Japan, the ¶Department of Cellular Function, Division of Cellular and Molecular Pathology, Niigata University Graduate School of Medical and Dental Sciences, Niigata 951-8510, Japan, and ‖Perseus Proteomics Inc., Tokyo 153-0041, Japan

⌘ *Author's Choice*—Final version full access.

Received October 17, 2011, and in revised form, January 16, 2012

Published, MCP Papers in Press, January 25, 2012, DOI 10.1074/mcp.M111.015073

[1] The abbreviations used are: PTX3, pentraxin 3; AZU1, azurocidin 1; GO, Gene Ontology; NET, neutrophil extracellular trap; MPO, myeloperoxidase; PMA, phorbol myristate acetate; PRR, pattern recognition receptor.

fined as the systemic inflammatory response syndrome, and a concomitant anti-inflammatory phase, referred to as the compensatory anti-inflammatory response syndrome. The pro-inflammatory response is initiated by the PRRs in immune cells recognizing molecules originating from infectious pathogens termed pathogen-associated molecular patterns and from inflammatory cells or tissues known as damage-associated molecular patterns (10). PTX3, a soluble PRR, has been shown to bind certain pathogens, complement components, and even to other PRRs in a calcium ion-dependent or -independent manner (1, 2). In addition to its pro-inflammatory activity, PTX3 also has been shown to play a role in protecting against severe inflammatory reactions, such as animal sepsis models (11), seizure-induced neurodegeneration (12), and acute myocardial infarction (13). As a marker of sepsis, plasma PTX3 exhibits a good correlation with mortality (7). An *in vivo* study showed that PTX3 transgenic mice are resistant to endotoxic shock and polymicrobial sepsis (11). Although negative feedback mediation of inflammation has been postulated (14), the actual roles of PTX3 in sepsis are not fully understood.

One of the approaches to the understanding of the mechanisms is the proteomic identification of the specific PTX3 ligands. The MS-based clinical proteomics approach is widely used both as a biomarker discovery and for verification purposes (15). However, it is generally considered that extensive fractionation is required to identify a new biomarker in biofluids (16) because of the wide dynamic range of proteins in blood and biofluids (17). On the other hand, affinity purification together with the MS strategy is a feasible approach to the identification of protein interactions, which combines tagged protein purification and quantitative proteomics using protein stable isotope labeling (18, 19). Here again, however, there are also technical difficulties in practically adapting this strategy to the clinical setting such as sepsis. One of the solutions to these technical barriers is the usage of antibodies. Immunopurification enables isolation of the protein of interest in a simple and effective way. In fact, antibody-based proteomics has been used in the discovery and confirmation of biomarkers in cancer (20). Thus, to better understand the molecular mechanisms of PTX3, we investigated PTX3 ligands by immunopurification of native PTX3 from septic patient fluids and shotgun proteomics for label-free relative quantitation. From the proteomic analysis, we found novel interactants, including some of the components of NETs, as well as known PTX3 ligands such as complement and extracellular matrix proteins. Further investigation revealed that azurocidin 1 (21), a bactericidal protein that localizes to NETs, was one of these direct PTX3 interacting partners that act through the oligomer N-terminal domain of PTX3 in a calcium ion-dependent manner. The interaction between PTX3 and components of NETs might play a protective role in sepsis. This strategy of targeted proteomics provides a useful method for detecting low levels of diagnostic biomarkers.

EXPERIMENTAL PROCEDURES

Reagents and Antibodies—Recombinant human azurocidin 1 and recombinant human myeloperoxidase were purchased from R & D Systems, Inc. Native human complement C1q was purchased from Merck. Mouse monoclonal antibody PPZ-1228 (IgG2b) against PTX3 that was generated as previously described (22) was used for immunopurification, immunoblotting, and binding assay. A horseradish peroxidase conjugation to PPZ-1228 was performed using a peroxidase labeling kit with NH_2 (Dojindo Laboratories) according to the manufacturer's instructions. Pooled human serum and heparin plasma were purchased from COSMO BIO Co., Ltd. The mouse monoclonal antibody Z6718 (IgG1) against azurocidin 1 was raised in our laboratory by immunizing mouse with recombinant human azurocidin 1.

Clinical Samples—Venous blood samples were drawn from patients with sepsis ($n = 9$, 73.2 ± 11.4 years old) in the emergency department on admission and were stored at −70 °C for less than 3 years until analysis. Culture studies, including blood, urine, sputum, and stool, were performed. This study was certified by the ethics committees of both Juntendo University and the University of Tokyo.

Immunopurification of PTX3 Complex from Patient Fluids—Antibody-cross-linked protein G-conjugated magnetic beads were prepared as previously described (23). Before immunopurification, sample fluid (1 ml/immunopurification) was thawed on ice and centrifuged for 5 min at 800 × *g*, and the pellet was discarded. Supernatant was passed through a 0.45-μm filter, exchanged to PBS using a PD-10 desalting column (GE Healthcare), added at the final concentration of 0.1% Nonidet P-40, and finally incubated with 0.5 mg of the antibody-cross-linked protein G-conjugated magnetic beads for 30 min at room temperature. Magnet beads were washed three times with PBS/0.1% Nonidet P-40 and once with PBS at room temperature. The affinity-purified proteins were eluted by 0.05% RapiGest (Waters) in 50 mM NH_4HCO_3 buffer for 30 min at 67 °C. Eluent was concentrated with 10% ice-cold TCA, washed with ice-cold acetone, and dried. All of the magnetic bead procedures of affinity purification were carried out with a Magnatrix 1200 (Precision System Science) magnetic bead reaction system.

Liquid Chromatography-Tandem Mass Spectrometry—In-solution digestion was carried out as previously described (23). A capillary reverse phase HPLC-MS/MS system (ZAPLOUS system; AMR Inc.) that was comprised of a Paradigm MS4 quadra solvent delivery system (Michrom BioResources), an HTC PAL autosampler (CTC Analytics), and LTQ Orbitrap XL ETD mass spectrometers (Thermo Scientific) equipped with an XYZ nanoelectrospray ionization source (AMR Inc.) was used for LC/MS/MS. Aliquots of the trypsinized samples were automatically injected into a peptide CapTrap cartridge (2.0 × 0.5-mm inner diameter; Michrom BioResources) attached to an injector valve for desalting and concentrating the peptides. After washing the trap with 98% H_2O, 2% ACN, 0.2% TFA, the peptides were loaded onto a separation capillary reverse phase column (Monocap C18 150 × 0.2-mm inner diameter; GL-Science) by switching the valve. The eluents used were: A, 98% H_2O, 2% ACN, 0.1% HCOOH, and B, 10% H_2O, 90% ACN, 0.1% HCOOH. The column was developed at the flow rate of 1.0 μl/min, with a concentration gradient of ACN: from 5% B to 35% B for 100 min, from 35% B to 95% B for 1 min, then sustained at 95% B for 9 min, from 95% B to 5% B for 1 min, and finally re-equilibrated with 5% B for 9 min. Effluents were introduced into the mass spectrometer via the nanoelectrospray ion interface that held the separation column outlet directly connected with an nanoelectrospray ionization needle (PicoTip FS360-50-30; New Objective Inc.). The ESI voltage was 2.0 kV, and the transfer capillary of the LTQ inlet was heated to 200 °C. No sheath or auxiliary gas was used. The mass spectrometer was operated in a data-dependent acquisition mode, in which the MS acquisition with a mass

range of *m/z* 420–1600 was automatically switched to MS/MS acquisition under the automated control of Xcalibur software. The top four precursor ions were selected by an MS scan with Orbitrap at a resolution of $r = 60{,}000$ for the subsequent MS/MS scans by ion trap in the normal/centroid mode, using the automated gain control mode with automated gain control values of 5.00×10^5 and 1.00×10^4 for full MS and MS/MS, respectively. We also employed a dynamic exclusion capability that allows the sequential acquisition of the MS/MS of abundant ions in the order of their intensities with an exclusion duration of 2.0 min and exclusion mass widths of −5 and +5 ppm. The trapping time was 100 ms with the auto gain control on.

Database Searching, Data Compilation, and Relative Quantitation—For the purpose of peptide identification, MS/MS data were processed with Mascot® software (version 2.2 Matrix Science) against the SwissProt 2010 *Homo sapiens* database (20,350 entries), assuming trypsin as the digestion enzyme and allowing for trypsin specificity of up to two missed cleavages. The database was searched with a peptide mass tolerance of 3 ppm and fragment mass tolerance of 0.8 Da, taking into account the fixed peptide modification by iodoacetamide derivative of cysteine, variable peptide modifications by the homoserine lactone of methionine, oxidation of methionine, acetylation of the N terminus, carbamidomethylation of methionine, and phosphorylation of tyrosine.

Scaffold software (version Scaffold_2_06_02; Proteome Software Inc.) was used for peptide/protein identification and relative quantitation. Peptide identifications were accepted if they could be established at greater than 95.0% probability as specified by the Peptide Prophet algorithm (24). Protein identifications were accepted if they could be established at greater than 99.0% probability and contained at least two identified peptides. Protein probabilities were assigned by the Protein Prophet algorithm (25). These identification criteria typically established a <0.01% false discovery rate, based on a decoy database search strategy (26). Proteins that contained similar peptides and could not be differentiated based on MS/MS analysis alone were grouped to satisfy the principles of parsimony. Label-free relative protein quantifications were performed using normalized spectral counts based on the total number of spectra identified in each sample. Quantification of different proteins that contained similar peptides was performed when an identical peptide was identified on individual entries using Scaffold software. We calculated the fold change value from the ratio of the normalized spectral counts of anti-PTX3 immunopurification to the normalized spectral counts of mouse IgG immunopurification in each sample. We extracted the candidate proteins if its unique peptide number was ≥2 and the fold change value was ≥2 in at least one sample.

Gene Ontology Analysis—The Gene Ontology terms were analyzed with DAVID Gene Functional Analysis tools (http://david.abcc.ncifcrf.gov/). We defined the significant enriched terms as proteins ≥5 in Fig. 2 and p value $\leq 1 \times 10^{-7}$.

Binding Assay—Polystyrene 96-well plates were immobilized with 50 μl/well of 1.0 μg/ml of each protein in TBS overnight at 4 °C. The plates were blocked with 100 μl/well of 1% BSA in TBS, 0.1% Triton X-100 for 2 h at room temperature. As the primary reaction, 50 μl of recombinant PTX3 diluted with 1% BSA in TBS with 0.1% Triton X-100 was added to each well and reacted for 1 h at room temperature. As a secondary reaction, 50 μl/well of horseradish peroxidase-conjugated anti-PTX3 antibody PPZ-1228 or horseradish peroxidase-conjugated anti-Myc antibody (9E10; Santa Cruz Biotechnology, Inc.) diluted with 1% BSA in TBS, 0.1% Triton X-100 was added and reacted for 1 h at room temperature. The plates were developed with 50 μl/well of 3,3′,5,5′-tetramethylbenzidine-soluble reagent for 30 min at room temperature and stopped with 50 μl/well of 3,3′,5,5′-tetramethylbenzidine stop buffer. Absorbance was read at 450/630 nm. Before each reaction, the plates were washed briefly with TBS, 0.1% Triton X-100. For the confirmation of calcium-dependent binding, 4 mM $CaCl_2$ or 4 mM EDTA were added to all of the buffers. Statistical analysis was performed using p values calculated by Student's t test.

Surface Plasmon Resonance Measurement—All of the surface plasmon resonance experiments were performed using a BIAcore 3000. Immobilization of recombinant PTX3 on the sensor chip CM5 was performed with an amine coupling kit using a standard coupling protocol. The reaction conditions were set at 5 μl/min at 25 °C using HBS-P with 0.5 M NaCl (10 mM HEPES, pH 7.4, 500 mM NaCl, and 0.005% Tween 20) as the running buffer. All of the flow cell surfaces were activated by a 1:1 mixture of 1-ethyl-3-[3-dimethylaminopropyl]-carbodiimide hydrochloride/*N*-hydroxysuccinimide for 7 min. Next, 100 μg/ml of recombinant PTX3 diluted with 10 mM sodium acetate, pH 3.6, was injected for 7 min. Deactivation of excess reactive groups was carried out by a 7-min injection of ethanolamine. One flow cell was left uncaptured in the samples used as a control. Approximately 4,000 RU of recombinant PTX3 was coupled by this method. For the kinetics analysis, five 2-fold dilutions of recombinant azurocidin 1 beginning at 135 nM were analyzed for 2 min of association followed by 2 min of dissociation. Regeneration of the surface was achieved by an injection of 10 μl of 1 M sodium acetate, pH 7.2, followed by 10 μl of 10 mM NaOH. For the confirmation of calcium-dependent binding, the HBS-P with 0.5 M NaCl buffers had 2 mM $CaCl_2$ or 3 mM EDTA added during the kinetic analysis. Kinetics were calculated using BIAeval software.

Cloning, Expression, and Purification of Recombinant PTX3—Recombinant nontagged human PTX3 was expressed and purified as previously described (22). For mammalian expression of tagged human PTX3 fragments, the coding sequences of the N-terminal domain of PTX3 (1–178 amino acids of hPTX3), C-terminal domain of PTX3 (179–381 amino acids of hPTX3) with an adaptation of the N-terminal signal sequence of PTX3 (1–17 amino acids of hPTX3), and full-length PTX3 (1–381 amino acids of hPTX3) were amplified and recloned into the NotI/XbaI site of a pEF4/Myc-His B vector (Invitrogen). The resulting expression vectors were transfected into FreeStyle™ Chinese hamster ovary S cells (Invitrogen) suspended in Invitrogen FreeStyle™ Chinese hamster ovary medium using FreeStyle™ MAX reagent (Invitrogen), and stably transfected cells were selected in expression medium containing 0.5 mg/ml Zeocin™ (Invitrogen). The clarified cell culture supernatants were purified using HisTrap HP 1-ml columns (GE Healthcare Life Sciences) according to the manufacturer's instructions.

For bacterial expression of tagged N-terminal domain human PTX3, the coding sequence of the N-terminal domain of PTX3 (18–178 amino acids of hPTX3) that adapted the tobacco etch virus (TEV) protease sequence (ENLYFQG) in the N-terminal, as well as a mutant sequence in which the cysteine residues at positions 47, 49, and 103 were changed to serine residues, were obtained from GenScript by optimizing these codons for effective expression. These were amplified and recloned into the NdeI/XhoI site of a pCold II vector (Takara Bio Inc.). The resulting expression vectors were transformed into BL21-CodonPlus-RIL cells (Agilent Technologies) and expressed according to the manufacturer's instructions. Collected cells were lysed with BugBuster® protein extraction reagents (Merck). The lysates were purified using HisTrap HP 1-ml columns (GE Healthcare Life Sciences) according to the manufacturer's instructions.

Cell Culture, Transient Transfection, Neutrophil Isolation, and Immunofluorescence—COS-1 cells were grown in DMEM supplemented with 10% fetal bovine serum. The expression plasmid of human azurocidin 1 (accession number NM_001700.3) was purchased from Origine Technologies, Inc. Transfection was performed using FuGENE 6 (Roche Applied Science) according to the manufacturer's instructions. HL-60 cells were grown in RPMI1640 supple-

TABLE I
Summary of PTX3 recovery from patient fluids

Patient no.	PTX3 recovery (ng)[a]		
	Heparin plasma	EDTA plasma	Serum
1		43	21
2		1.4	0.2
3	8.4	2.0	
4	1.3	0.5	1.2
5	11	12	15
6	27	21	28
7	24	20	15
8	<1.0	<1.0	<1.0
9	1.8	1.6	1.8
Spike (200 ng/ml)[b]	11		11

[a] PTX3 recovery was calculated from the immunoblotting of the purified fractions (supplemental Fig. 1).

[b] Artificial samples were pooled normal plasma and serum spiked with 200 ng/ml of recombinant PTX3.

mented with 10% fetal bovine serum. The induction of differentiation into the neutrophil lineage was performed with 10 μM of all-*trans* retinoic acid treatment for 4 days. Neutrophils were isolated as previously described (27). Immunofluorescence was performed as previously described (23, 28). Briefly, isolated neutrophils were suspended on glass slide chambers treated with poly-L-lysine (Sigma) in RPMI 1640 medium with 2% fetal bovine serum. After culturing for 1 h, the neutrophils were stimulated with 20 ng/ml of phorbol myristate acetate (PMA) for 40 min. The specimens were fixed with 4% paraformaldehyde for 5 min, permeabilized with 0.5% Triton X-100 for 5 min, and blocked with 10% normal goat serum for 30 min. These were stained with monoclonal antibodies anti-PTX3 PPZ-1228 and monoclonal antibodies anti-azurocidin 1 Z6718 labeled with a Zenon Alexa Fluor 488 labeling kit (Invitrogen) in dilutions of 1:50 and 1:500, respectively. For the detection of PPZ-1228, the Alexa Fluor 568 anti-mouse IgG Fab′ fragment (1:250 dilution; Invitrogen) was used as a secondary antibody. Immunofluorescence was captured using confocal laser scanning microscopy (LSM510META; Carl Zeiss).

RESULTS

Immunopurification of Circulating PTX3 Complexes in Patients with Sepsis—For the isolation of the circulating PTX3-interacting proteins, the native PTX3 complexes were immunopurified from the blood of the septic patients for the subsequent application of shotgun proteomics. To evaluate the interacting proteins circulating in the blood in a rigorous fashion, several different blood sampling conditions were utilized. Thus, heparin plasma, EDTA plasma, and serum were obtained from each septic patient, although the entire fluid set was not completed for certain patients. The septic patient characteristics are shown in supplemental Table 1. The final diagnoses included two with acute pan peritonitis and one each with bacterial pneumonia, acute pyelonephritis, cellulitis, acute cholangitis, pyorrhea, acute bacterial colitis, and acute exacerbation of intestinal pneumonitis. Four patients died within 28 days. In addition to patient fluids, the artificially high PTX3 concentration samples obtained by spiking 200 ng/ml of recombinant PTX3 into the pooled normal plasma and serum were analyzed for reference. The immunopurification of the native protein complexes was based on a highly sensitive immunoprecipitation system we developed, as reported (23).

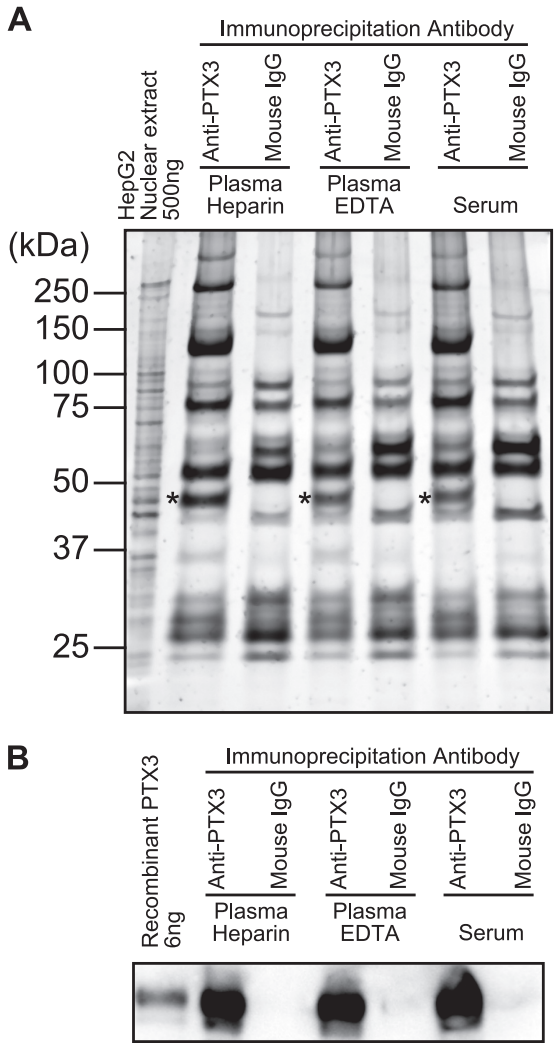

FIG. 1. **Immunopurification quality check of the PTX3 complexes from septic patient fluids.** Immunopurified PTX3 and its interactants from the fluids of patient 6 (see Table I and supplemental Table 1) were stained with SYPRO Ruby protein staining (*A*) and immunoblotted with horseradish peroxidase-conjugated anti-PTX3 antibody PPZ-1228 (*B*). The *bands* marked with *asterisks* in *A* indicate PTX3.

Samples were immunoprecipitated with antibody-cross-linked protein G-conjugated magnetic beads. Part of the immunoprecipitation procedure was automated to obtain stable recovery. The immunoprecipitated fractions were eluted in the liquid phase and concentrated using the TCA-acetone precipitation method. After immunopurification with the anti-PTX3 monoclonal antibody, portions of the purified fraction were analyzed by immunoblotting with the anti-PTX3 antibody for confirmation of both the recovery and specificity (Table I and supplemental Fig. 1). The recovery of PTX3 from 1.0 ml of each sample was in the range of 1–40 ng. From the results of the protein staining and immunoblotting of the purified fractions, the purification quality was regarded as sufficiently high to carry out shotgun proteomics (Fig. 1).

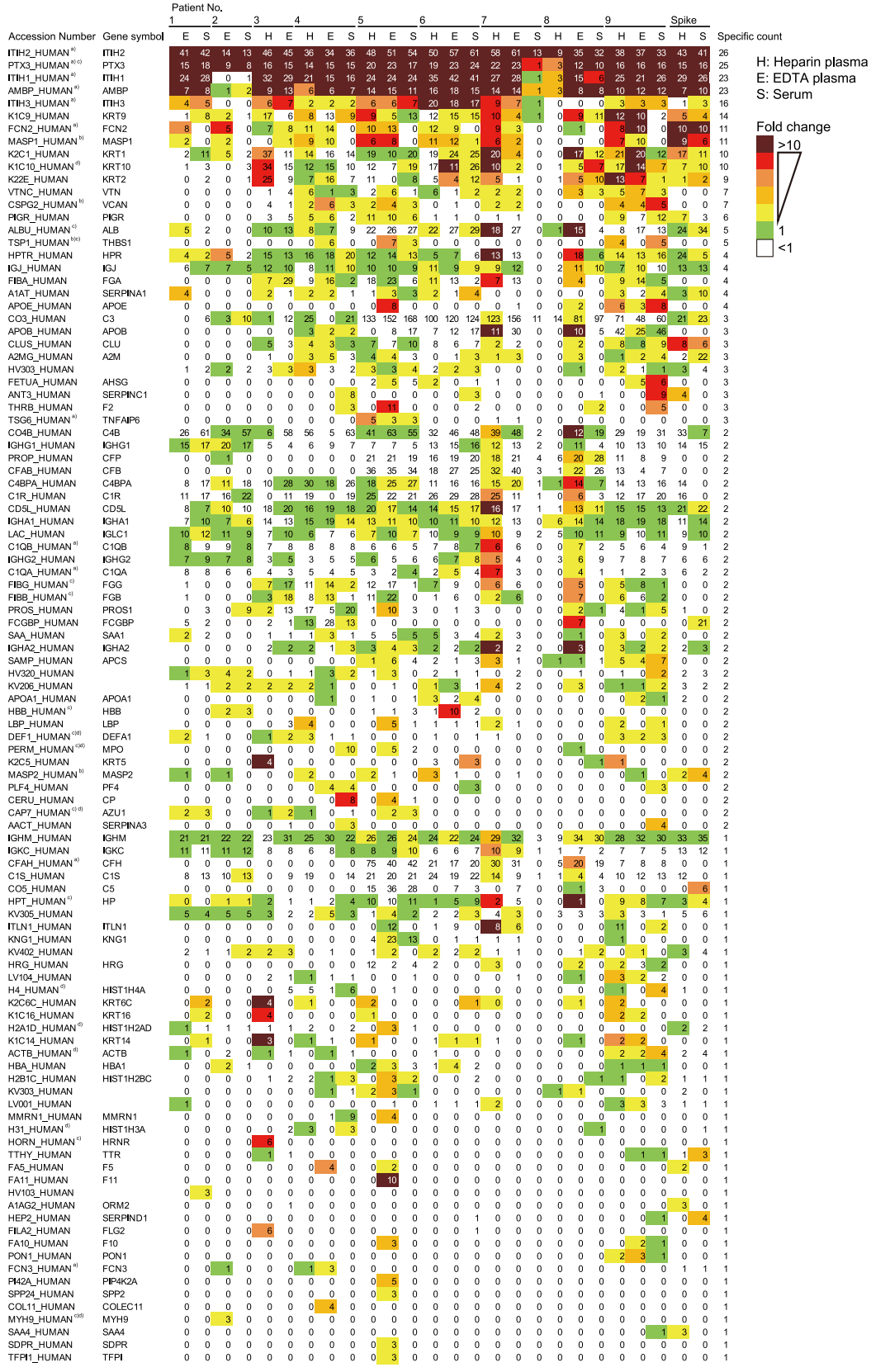

10.1074/mcp.M111.015073–5

Proteomic Profile of Circulating PTX3 Complexes in Sepsis—Shotgun proteomics analysis was performed using these purified PTX3 complex fractions. From the identification data obtained, 104 proteins regarded as PTX3-interacting protein candidates were extracted using label-free relative quantitation via spectral counting (19, 26) (Fig. 2 and supplemental Table 2). Among these proteins, the known PTX3 ligands and PTX3 ligand-interacting proteins, such as complement components and extracellular matrix proteins, were included (Fig. 2 and supplemental Table 3). Notably, certain proteins were found that are components of neutrophil granules (29) and NETs (30) (Fig. 2 and supplemental Table 3). Next, we applied Gene Ontology (GO) term analysis to check whether some of the biological terms were significantly enriched in the extracted proteins (Fig. 3, *A* and *B*, and supplemental Table 4). Analysis of enriched GO biological process terms showed a significant enrichment of the known PTX3 functions, such as those related to the regulation of inflammation and immunity (Fig. 3*A*). Additionally, functions related to protection against sepsis, such as the response to wounding and coagulation, were also observed (Fig. 3*A*). Consistent with our observation that the extracted protein contained components of neutrophil granules and NETs, the analysis of the enriched GO cellular components terms showed that the localizations of the extracted proteins were mainly the extracellular space and granule (Fig. 3*B*). Taken together, the proteomic profile of the PTX3 complexes in these septic patients included protein components of NETs, as well as the known PTX3 ligands, such as complement and extracellular matrix component proteins (Fig. 3*C*).

Identification of Specific Interaction of Azurocidin 1 to PTX3—To evaluate the direct binding of the newly identified candidate proteins to PTX3, an ELISA-based binding assay using recombinant proteins was performed. We have checked 12 proteins, some of which were either neutrophil granule proteins or NETs proteins. We observed that AZU1 and myeloperoxidase (MPO) exhibited high affinity binding signals to PTX3 (Fig. 4*A*), although the binding signals of the other proteins we checked for affinity to PTX3 were very low (supplemental Fig. 2). Thus, we further checked the effect of the calcium ion dependence of these two proteins on PTX3 binding. The data showed that AZU1 clearly exhibited calcium ion-dependent binding, whereas MPO did not require calcium ions to bind to PTX3 (Fig. 4*B*). For additional confirmation of the calcium ion-dependent binding of AZU1-PTX3, real time biomolecule interaction analysis using surface plasmon resonance measurement was performed. This result also clearly showed the calcium ion-dependent binding signal of AZU1-PTX3, with a calculated K_D of 22 $\pm$ 7.6 nM (Fig. 4*C*).

Characterization of the PTX3 Elements Involved in the Binding to Azurocidin 1—The PTX3 structure is divided into two functional domains: a pentraxin-like domain in its C terminus and another, long domain in its N terminus (1). Some PTX3 ligands require full-length PTX3 for binding, whereas others exhibit PTX3 domain-specific binding (1). Thus, we prepared N-terminal and C-terminal PTX3 fragment proteins (Fig. 5*A*) to identify the PTX3 domain responsible for binding to AZU1. The multimeric forms of each protein with interdisulfide bonds (Fig. 5*B*) were consistent with a previous report (31). The binding assay showed that AZU1 predominantly bound to the N-terminal domain of PTX3 (Fig. 5*C*). Myeloperoxidase exhibited binding signals in both the N-terminal and C-terminal domains of PTX3, but the C-terminal domain exhibited a relatively lower signal (Fig. 5*C*). We further checked the oligomer effect of the N-terminal domain of PTX3 on AZU1 binding using cysteine residue-mutated protein (Fig. 6*A*). Fibroblast growth factor 2, which is a protein that interacts through the N-terminal domain of PTX3 like AZU1, reportedly abolishes the binding activity to the PTX3 N-terminal domain when this N-terminal domain PTX3 loses its interdisulfide bonds (31). The oligomer formations in each protein with interdisulfide bonds (Fig. 6*B*) were also consistent with a previous report (31). The result showed that the N-terminal domain of a PTX3 mutant, in which the cysteine residues at positions 47, 49, and 103 were changed to serine residues, dramatically loses the binding signal to AZU1 (Fig. 6*C*).

Co-localization of PTX3 and Azurocidin 1 in Neutrophil Granules and NETs—Finally, to check the binding of AZU1-PTX3 in the NETs, we performed an immunofluorescence analysis. For this immunofluorescence, we generated a monoclonal antibody against AZU1 and checked the specificity by immunoblotting. The monoclonal antibody displayed specific detection of full-length AZU1 overexpressed in mammalian cells (Fig 7*A*, *left panel*), HL-60 cells differentiated into a neutrophil lineage (Fig 7*A*, *center panel*), and neutrophils (Fig 7*A*, *right panel*). We also observed an increasing AZU1 content in the neutrophil culture supernatant stimulated by PMA (Fig 7*A*, *right panel*). Partial co-localization of AZU1 and PTX3 was observed upon checking the NETs from the neutrophils stimulated with PMA (Fig. 7*B*).

FIG. 2. **Proteomic results for PTX3 complexes in septic patients.** Identified proteins regarded as the candidates of PTX3 complexes (unique peptide number ≥2 and fold change value ≥2 in at least one sample) are shown. The complete lists of identified proteins are shown in supplemental Table 2. The *number* shown for each protein represents the unique peptide number, and the *colored boxes* for each protein represent the fold change value from the ratio of the normalized spectral counts of anti-PTX3 immunopurification to the normalized spectral counts of mouse IgG immunopurification, respectively. Proteins were sorted by the times regarded as specific (specific counts). *a)*, reported PTX3-interacting proteins. *b)*, ficolins or tumor necrosis factor-inducible gene 6 protein-interacting proteins. *c)*, components of neutrophil granules. *d)*, components of neutrophil extracellular traps. *a)–d)*, details are provided in supplemental Table 3.

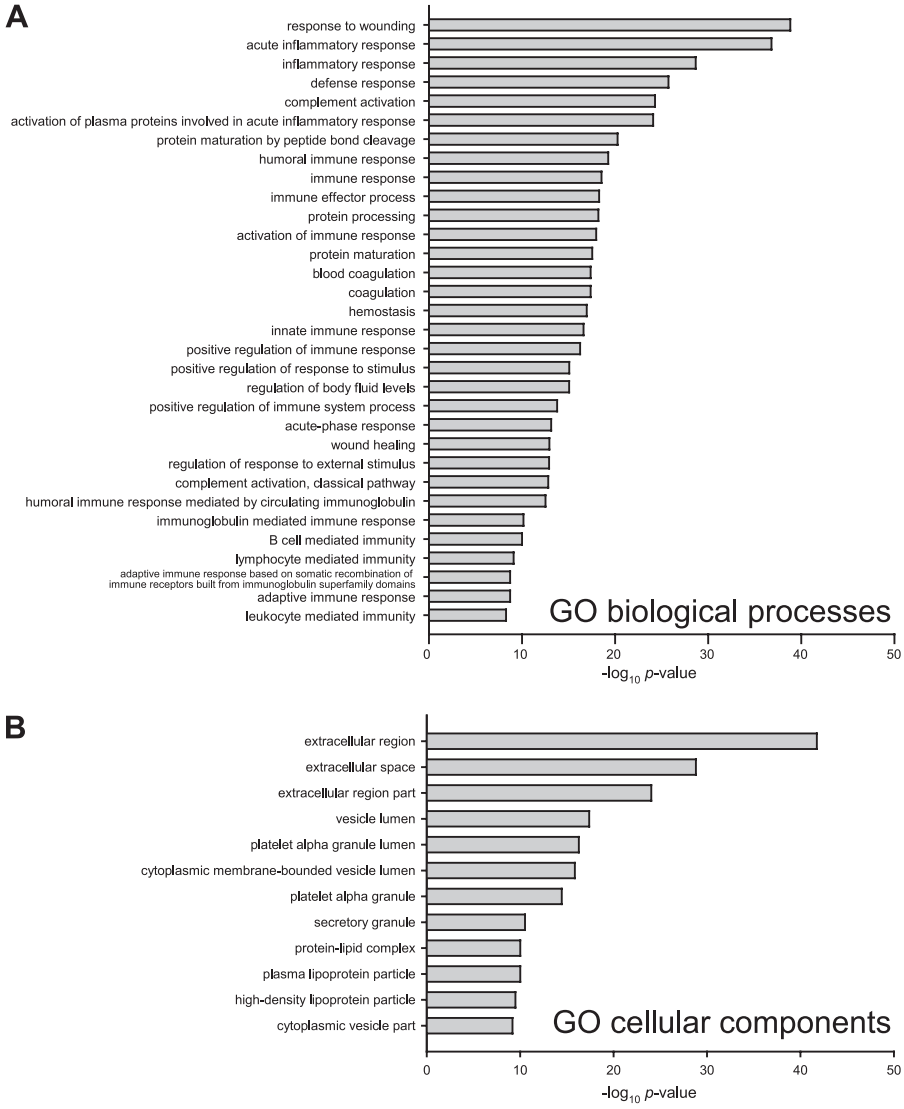

FIG. 3. **Functional classification of PTX3 complexes in septic patients.** The enriched Gene Ontology terms among the PTX3 interactants extracted in Fig. 2 were analyzed with DAVID gene functional analysis tools (http://david.abcc.ncifcrf.gov/). *A* and *B*, Gene Ontology biological processes (*A*) and Gene Ontology cellular components (*B*) are shown. The detailed results are provided in supplemental Table 4. *C*, schematic representation of the PTX3 functional complexes in septic patients. Portions of the identified PTX3 ligands in Fig. 2 were classified in terms of their functions according to review (1). The *asterisks* indicate the identified proteins listed in Fig. 2.

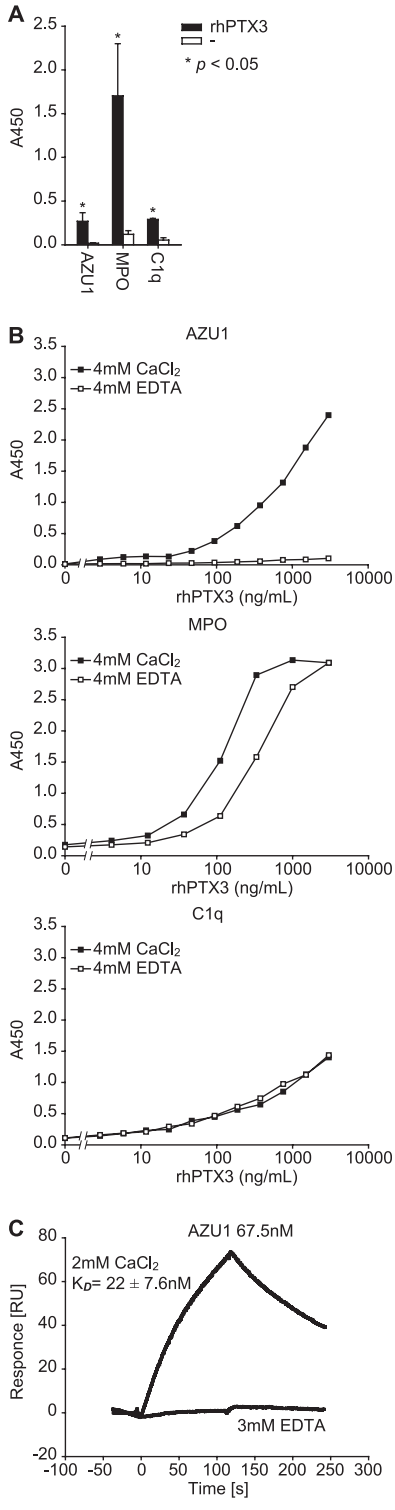

FIG. 4. **Interaction analysis of PTX3 with azurocidin 1 and myeloperoxidase.** *A*, binding assay of 100 ng/ml recombinant PTX3 (*rhPTX3*) to immobilized AZU1, MPO, and C1q as the control. The detection antibody was horseradish peroxidase-conjugated anti-PTX3 antibody PPZ-1228. All of the assay buffers contained 4 mM $CaCl_2$. The data are from three independent experiments of duplicate wells. *B*, binding assay of recombinant PTX3 to immobilized AZU1 (*top panel*), MPO (*middle panel*), and C1q as the control (*bottom panel*) for calcium ion dependence. The detection antibody was horseradish peroxidase-conjugated anti-PTX3 antibody PPZ-1228. All of the assay buffers contained 4 mM $CaCl_2$ (*closed squares*) or 4 mM EDTA (*open squares*). The data are representative of two experiments. *C*, surface plasmon resonance measurement of the binding of 67.5 nM AZU1 to immobilized recombinant PTX3 with calcium ion dependence. Running buffers contained 2 mM $CaCl_2$ or 3 mM EDTA. The data are representative of two experiments. Calculated affinity was from two experiments of five 2-fold dilutions of AZU1 beginning at 135 nM in the presence of calcium ions.

DISCUSSION

One of the challenges in establishing diagnostic or therapeutic biomarkers has been how to analyze whole plasma proteins on the order of ng/ml or even pg/ml concentrations. Despite the development of highly sensitive MS methods, it is still very difficult to detect the most minor components of plasma proteins. We have been steadily working to establish an antibody-based proteomics method to determine complexes of nuclear proteins (23). We applied this method to an analysis of the PTX3 complex in septic plasma and serum using a specific monoclonal antibody (Fig. 1). PTX3, which is undetectable in healthy plasma (<2 ng/ml) (6) and is known to be elevated to as high as 200 ng/ml in sepsis, with the increase is clearly related to the severity of the disease (7). Many biomarkers of sepsis have been identified, but they have neither the specificity or sensitivity required for clinical practice (32). In this study, the goal was to find new diagnostic biomarker candidates associated with PTX3, which act in the innate immune response in sepsis.

The result of proteomic analysis of the PTX3 complexes mainly contained the known PTX3 ligands, such as the inter-α-trypsin inhibitors (33), ficolins (34), tumor necrosis factor-inducible gene 6 protein (35), and complement C1q (36) (Fig. 2 and supplemental Table 3). These components play a role in activities such as complement activation, inflammation regulation, and extracellular matrix deposition. Among the other identified proteins, we found mannan-binding lectin serine protease 1 and 2 (MASP1 and MASP2), versican core protein (VCAN), and thrombospondin-1 (THBS1) (Fig. 2). MASP1 and MASP2 are reported to be ficolin-interacting proteins (34), whereas VCAN and THBS1 are tumor necrosis factor-inducible gene 6-interacting proteins (35) (supplemental Table 3). These proteins may indirectly interact with PTX3. The known PTX3 ligands are likely to be stable, because most were also identified in the spiked samples. Nevertheless, these ligands could exert synergistic effects together with PTX3 in sepsis.

Because we used whole IgG molecule for isolation, we were not able to eliminate the possible association of IgG-interacting proteins, such as complement. We have listed complement as a PTX3-interacting protein, because it is reported to be a ligand of PTX3 (36), and there was an increased fold change value. The fluctuation of the albumin score observed here is attributed to the unstable contamination, which took

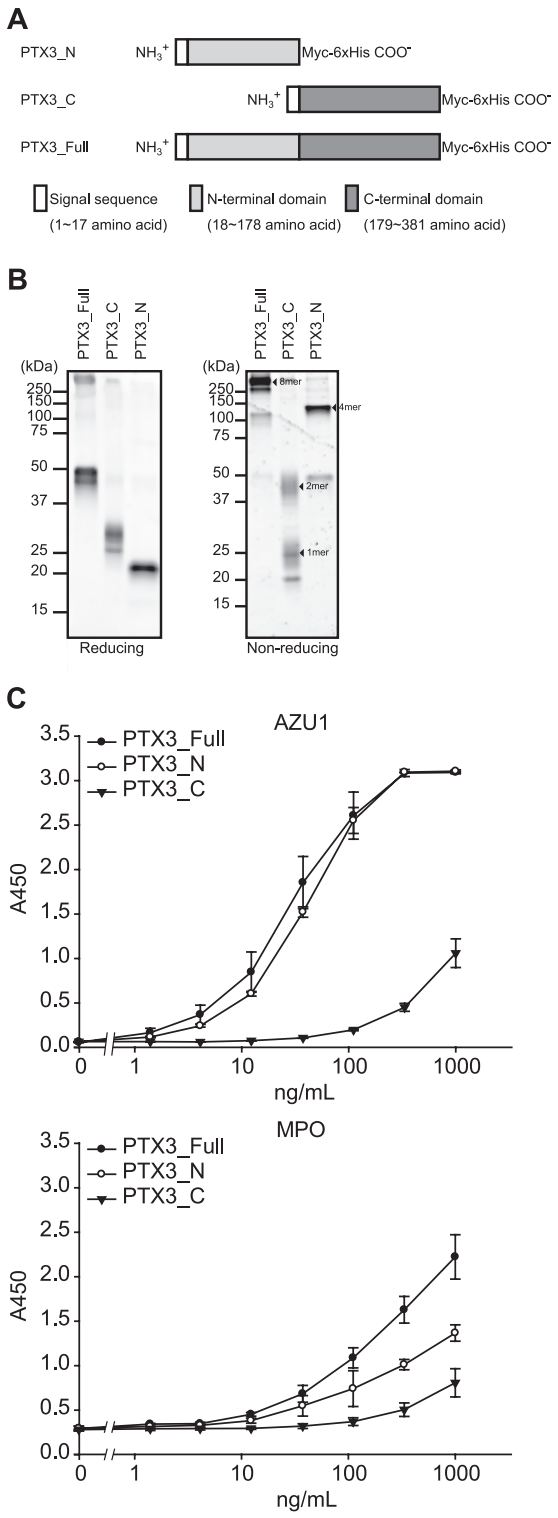

FIG. 5. **Identification of the PTX3 domain responsible for the interaction with azurocidin 1.** *A*, schematic representation of the PTX3 fragments. The N-terminal domain (*PTX3_N*), the C-terminal domain (*PTX3_C*), and the full length (*PTX3_Full*) of human PTX3 with Myc-His_6-tagged proteins were expressed by mammalian cells. *B*, CYPRO Ruby staining of purified proteins with reducing and nonreducing conditions. *C*, binding assay of the PTX3 fragments to immobilized AZU1 and MPO. The detection antibody was horseradish peroxidase-conjugated anti-Myc antibody. All of the assay buffers contained 4 mM $CaCl_2$. The data are from three independent experiments of duplicate wells.

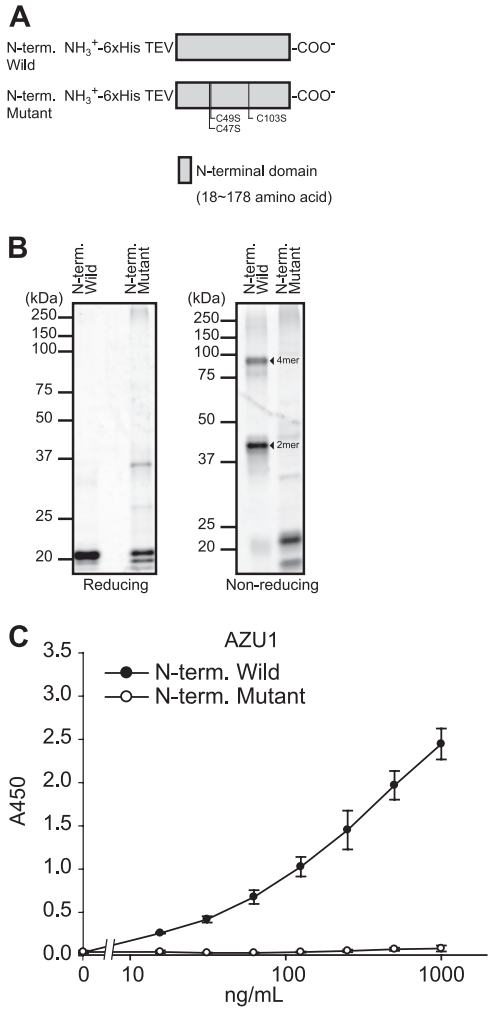

FIG. 6. **Effect of N-terminal domain PTX3 oligomer formation for binding to azurocidin 1.** *A*, schematic representation of the PTX3 N-terminal domain (*N-term. Wild*) and the N-terminal domain with all of the cysteine residues mutated (*N-term. Mutant*) with His_6 tobacco etch virus (TEV) protease sequence tagged proteins. These domains were expressed by bacterial cells. *B*, CYPRO Ruby staining of purified proteins with reducing and nonreducing conditions. *C*, binding assay of the N-terminal domain of PTX3 to AZU1 to show the PTX3 multimerized dependence. The detection antibody was horseradish peroxidase-conjugated anti-PTX3 antibody PPZ-1228. All of the assay buffers contained 4 mM $CaCl_2$. The data are from three independent experiments of duplicate wells.

place during the sample preparation, because the albumin is several orders of magnitude more abundant than the other proteins discussed here.

Interestingly, we additionally found some of the same components of the neutrophil granules and NETs as the PTX3-interacting candidates (Fig. 2). The analysis of the GO term

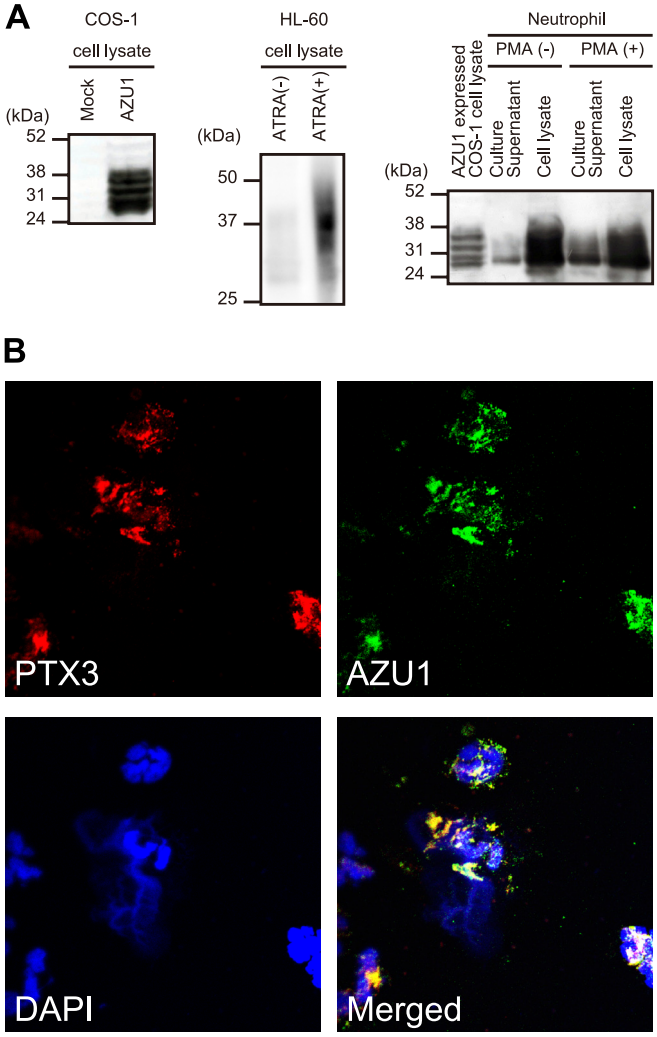

FIG. 7. **Co-localization of PTX3 and azurocidin 1 in neutrophil extracellular traps.** *A*, the specificity check of the anti-AZU1 monoclonal antibody Z6718 by immunoblotting. *Left panel*, overexpressed full-length AZU1 obtained by COS-1 cells. *Center panel*, HL-60 cells treated with all-*trans*-retinoic acid (*ATRA*). *Right panel*, neutrophil and its culture supernatant with and without PMA stimulation. *B*, localization of PTX3 and AZU1 in NETs by immunofluorescence. The released NETs induced by PMA stimulation were visualized with the anti-PTX3 monoclonal antibody PPZ-1228 (*red*) and the anti-AZU1 monoclonal antibody Z6718 (*green*). The specimens were also visualized with 4,6-diamidino-2-phenylindole (*DAPI*) staining (*blue*). The *right bottom panel* shows the merged image of the PTX3, AZU1, and DAPI staining.

also supported that, in addition to the known PTX3 functions and specifically the protective functions against sepsis, some of the identified proteins were associated with neutrophil granules and NETs (Fig. 3 and supplemental Table 4). This finding from the proteomic profile of the PTX3 complexes in sepsis suggests a role for PTX3 in the tethering of the NETs components so as to be able to recognize and kill pathogens effectively. Among them, both AZU1 and MPO, which are components of neutrophil granules and NETs (27), exhibited significant binding to PTX3 (Fig. 4*A*). The other candidate proteins we checked did not exhibit potent binding signals to PTX3 (supplemental Fig. 2), so these might be low affinity interaction proteins or indirect partners. AZU1 and MPO are direct PTX3-interacting protein candidates in sepsis, so we examined the binding mechanisms in detail. AZU1 exhibited calcium ion-dependent binding, which took place in a dose-dependent manner (Fig. 4*B*), and also high affinity binding (Fig. 4*C*) to PTX3. Furthermore, AZU1 binding required the PTX3 N-terminal domain oligomer, as was also the case for fibroblast growth factor 2 and PTX3 interaction (31) (Figs. 5 and 6). This result suggests a similar binding mechanism for these proteins.

Because the biochemical analysis clearly demonstrated the direct binding of AZU1 to PTX3, we checked whether PTX3 and AZU1 were associated in NETs. An anti-AZU1 monoclonal antibody that we raised was shown to specifically recognize the differently glycosylated exogenous AZU1 and native AZU1 in neutrophils (21, 37) (Fig. 7*A*). Although AZU1 is stored in azurophilic granules (38) and PTX3 is in specific granules (4), a portion of them co-localize in NETs (Fig. 7*B*). A previous study reported that PTX3 and MPO do not co-localize in neutrophil granules (4). Therefore, the PTX3-AZU1 and PTX3-MPO interactions would be expected to occur after the release from the granules or NETs. We could not clearly determine whether the circulating PTX3-AZU1 and -MPO complexes were of NETs origin or were formed in the plasma, and it is possible that PTX3 acts as a scaffold protein that interacts with both pathogens and bactericidal proteins such as AZU1 and MPO (21, 39, 40) at the inflammatory sites. Other component proteins of NETs (neutrophil defensin 1, histones, actin, myosin, and keratin) have also been identified as candidate PTX3-interacting partners in sepsis. (The details of the interaction pattern will be discussed elsewhere.) The plasma levels of AZU1 and MPO are significantly increased in septic patients (41, 42). The AZU1 level, however, does not closely correlate with mortality (43). Our observation here suggests that the plasma levels of the AZU1-PTX3 and/or MPO-PTX3 complexes are specific and sensitive markers of sepsis. By the specification of the PTX3 complex, it is possible to go to the validation study using a small volume of septic patient samples.

In conclusion, the proteomic profile of the PTX3 complexes in sepsis determined by means of an effective immunopurification method demonstrates that PTX3 interacts with the components of neutrophil granules and NETs. Among these, we confirmed the direct interactions of PTX3-AZU1 and PTX3-MPO. In particular, AZU1 and PTX3 exhibited partial co-localization in the NETs. These results suggest that PTX3, as a soluble PRR, might help form the anti-pathogenic microenvironment by tethering bactericidal proteins in sepsis. This interaction seems to both play a protective role against and also act as a biomarker of sepsis.

Acknowledgments—We thank Dr. Nobuchika Suzuki for kindly providing the HL-60 cell lysates. We thank Dr. Kevin Boru of Pacific Edit for review of the manuscript. We also acknowledge Chizuru Saruta, Rie Fukuda, Yoko Chikaoka, and Aya Nakayama for excellent technical assistance.

* This work was supported by Development of New Functional Antibody Technologies of the New Energy and Industrial Technology Development Organization (Japan); Grant-in-Aid for Scientific Research 20221010 from the Japanese Ministry of Education, Culture, Sports, Science and Technology; and collaborative research of the University of Tokyo and JSR Corporation. The costs of publication of this article were defrayed in part by the payment of page charges. This article must therefore be hereby marked "*advertisement*" in accordance with 18 U.S.C. Section 1734 solely to indicate this fact.

[S] This article contains supplemental material.

§§ To whom correspondence should be addressed: Research Center for Advanced Science and Technology, The University of Tokyo, 4-6-1 Komaba, Meguro, Tokyo 153-8904, Japan. Tel./Fax: 81-3-5452-5231; E-mail: hamakubo@lsbm.org.

REFERENCES

1. Bottazzi, B., Doni, A., Garlanda, C., and Mantovani, A. (2010) An integrated view of humoral innate immunity: Pentraxins as a paradigm. *Annu. Rev. Immunol.* **28,** 157–183
2. Mantovani, A., Garlanda, C., Doni, A., and Bottazzi, B. (2008) Pentraxins in innate immunity: From C-reactive protein to the long pentraxin PTX3. *J. Clin. Immunol.* **28,** 1–13
3. Garlanda, C., Bottazzi, B., Bastone, A., and Mantovani, A. (2005) Pentraxins at the crossroads between innate immunity, inflammation, matrix deposition, and female fertility. *Annu. Rev. Immunol.* **23,** 337–366
4. Jaillon, S., Peri, G., Delneste, Y., Frémaux, I., Doni, A., Moalli, F., Garlanda, C., Romani, L., Gascan, H., Bellocchio, S., Bozza, S., Cassatella, M. A., Jeannin, P., and Mantovani, A. (2007) The humoral pattern recognition receptor PTX3 is stored in neutrophil granules and localizes in extracellular traps. *J. Exp. Med.* **204,** 793–804
5. Brinkmann, V., Reichard, U., Goosmann, C., Fauler, B., Uhlemann, Y., Weiss, D. S., Weinrauch, Y., and Zychlinsky, A. (2004) Neutrophil extracellular traps kill bacteria. *Science* **303,** 1532–1535
6. Presta, M., Camozzi, M., Salvatori, G., and Rusnati, M. (2007) Role of the soluble pattern recognition receptor PTX3 in vascular biology. *J. Cell Mol. Med.* **11,** 723–738
7. Mauri, T., Bellani, G., Patroniti, N., Coppadoro, A., Peri, G., Cuccovillo, I., Cugno, M., Iapichino, G., Gattinoni, L., Pesenti, A., and Mantovani, A. (2010) Persisting high levels of plasma pentraxin 3 over the first days after severe sepsis and septic shock onset are associated with mortality. *Intensive Care Med.* **36,** 621–629
8. Martin, G. S., Mannino, D. M., Eaton, S., and Moss, M. (2003) The epidemiology of sepsis in the United States from 1979 through 2000. *N. Engl. J. Med.* **348,** 1546–1554
9. Rittirsch, D., Flierl, M. A., and Ward, P. A. (2008) Harmful molecular mechanisms in sepsis. *Nat. Rev. Immunol.* **8,** 776–787
10. Xiang, M., and Fan, J. (2010) Pattern recognition receptor-dependent mechanisms of acute lung injury. *Mol. Med.* **16,** 69–82
11. Souza, D. G., Soares, A. C., Pinho, V., Torloni, H., Reis, L. F., Teixeira, M. M., Dias, A. A., and Martins, M. T. (2002) Increased mortality and inflammation in tumor necrosis factor-stimulated gene-14 transgenic mice after ischemia and reperfusion injury. *Am. J. Pathol.* **160,** 1755–1765
12. Ravizza, T., Moneta, D., Bottazzi, B., Peri, G., Garlanda, C., Hirsch, E., Richards, G. J., Mantovani, A., and Vezzani, A. (2001) Dynamic induction of the long pentraxin PTX3 in the CNS after limbic seizures: Evidence for a protective role in seizure-induced neurodegeneration. *Neuroscience* **105,** 43–53
13. Salio, M., Chimenti, S., De Angelis, N., Molla, F., Maina, V., Nebuloni, M., Pasqualini, F., Latini, R., Garlanda, C., and Mantovani, A. (2008) Cardioprotective function of the long pentraxin PTX3 in acute myocardial infarction. *Circulation* **117,** 1055–1064
14. Deban, L., Russo, R. C., Sironi, M., Moalli, F., Scanziani, M., Zambelli, V., Cuccovillo, I., Bastone, A., Gobbi, M., Valentino, S., Doni, A., Garlanda, C., Danese, S., Salvatori, G., Sassano, M., Evangelista, V., Rossi, B., Zenaro, E., Constantin, G., Laudanna, C., Bottazzi, B., and Mantovani, A. (2010) Regulation of leukocyte recruitment by the long pentraxin PTX3. *Nat. Immunol.* **11,** 328–334
15. Parker, C. E., Pearson, T. W., Anderson, N. L., and Borchers, C. H. (2010) Mass-spectrometry-based clinical proteomics: A review and prospective. *Analyst* **135,** 1830–1838
16. Mallick, P., and Kuster, B. (2010) Proteomics: A pragmatic perspective. *Nat. Biotechnol.* **28,** 695–709
17. Anderson, N. L., and Anderson, N. G. (2002) The human plasma proteome: History, character, and diagnostic prospects. *Mol. Cell. Proteomics* **1,** 845–867
18. Gingras, A. C., Gstaiger, M., Raught, B., and Aebersold, R. (2007) Analysis of protein complexes using mass spectrometry. *Nat. Rev. Mol. Cell Biol.* **8,** 645–654
19. Kaake, R. M., Wang, X., and Huang, L. (2010) Profiling of protein interaction networks of protein complexes using affinity purification and quantitative mass spectrometry. *Mol. Cell. Proteomics* **9,** 1650–1665
20. Brennan, D. J., O'Connor, D. P., Rexhepaj, E., Ponten, F., and Gallagher, W. M. (2010) Antibody-based proteomics: Fast-tracking molecular diagnostics in oncology. *Nat. Rev. Cancer* **10,** 605–617
21. Watorek, W. (2003) Azurocidin: inactive serine proteinase homolog acting as a multifunctional inflammatory mediator. *Acta Biochim. Pol.* **50,** 743–752
22. Savchenko, A., Imamura, M., Ohashi, R., Jiang, S., Kawasaki, T., Hasegawa, G., Emura, I., Iwanari, H., Sagara, M., Tanaka, T., Hamakubo, T., Kodama, T., and Naito, M. (2008) Expression of pentraxin 3 (PTX3) in human atherosclerotic lesions. *J. Pathol.* **215,** 48–55
23. Daigo, K., Kawamura, T., Ohta, Y., Ohashi, R., Katayose, S., Tanaka, T., Aburatani, H., Naito, M., Kodama, T., Ihara, S., and Hamakubo, T. (2011) Proteomic analysis of native hepatocyte nuclear factor-4 (HNF4) isoforms, phosphorylation status, and interactive cofactors. *J. Biol. Chem.* **286,** 674–686
24. Keller, A., Nesvizhskii, A. I., Kolker, E., and Aebersold, R. (2002) Empirical statistical model to estimate the accuracy of peptide identifications made by MS/MS and database search. *Anal. Chem.* **74,** 5383–5392
25. Nesvizhskii, A. I., Keller, A., Kolker, E., and Aebersold, R. (2003) A statistical model for identifying proteins by tandem mass spectrometry. *Anal. Chem.* **75,** 4646–4658
26. Prokai, L., Stevens, S. M., Jr., Rauniyar, N., and Nguyen, V. (2009) Rapid label-free identification of estrogen-induced differential protein expression *in vivo* from mouse brain and uterine tissue. *J. Proteome Res.* **8,** 3862–3871
27. Savchenko, A. S., Inoue, A., Ohashi, R., Jiang, S., Hasegawa, G., Tanaka, T., Hamakubo, T., Kodama, T., Aoyagi, Y., Ushiki, T., and Naito, M. (2011) Long pentraxin 3 (PTX3) expression and release by neutrophils *in vitro* and in ulcerative colitis. *Pathol. Int.* **61,** 290–297
28. Sakamoto, A., Kawasaki, T., Kazawa, T., Ohashi, R., Jiang, S., Maejima, T., Tanaka, T., Iwanari, H., Hamakubo, T., Sakai, J., Kodama, T., and Naito, M. (2007) Expression of liver X receptor α in rat fetal tissues at different developmental stages. *J. Histochem. Cytochem.* **55,** 641–649
29. Lominadze, G., Powell, D. W., Luerman, G. C., Link, A. J., Ward, R. A., and McLeish, K. R. (2005) Proteomic analysis of human neutrophil granules. *Mol. Cell. Proteomics* **4,** 1503–1521
30. Urban, C. F., Ermert, D., Schmid, M., Abu-Abed, U., Goosmann, C., Nacken, W., Brinkmann, V., Jungblut, P. R., and Zychlinsky, A. (2009) Neutrophil extracellular traps contain calprotectin, a cytosolic protein complex involved in host defense against *Candida albicans*. *PLoS Pathog.* **5,** e1000639
31. Inforzato, A., Baldock, C., Jowitt, T. A., Holmes, D. F., Lindstedt, R., Marcellini, M., Rivieccio, V., Briggs, D. C., Kadler, K. E., Verdoliva, A., Bottazzi, B., Mantovani, A., Salvatori, G., and Day, A. J. (2010) The angiogenic inhibitor long pentraxin PTX3 forms an asymmetric octamer with two binding sites for FGF2. *J. Biol. Chem.* **285,** 17681–17692
32. Pierrakos, C., and Vincent, J. L. (2010) Sepsis biomarkers: A review. *Crit. Care* **14,** R15
33. Scarchilli, L., Camaioni, A., Bottazzi, B., Negri, V., Doni, A., Deban, L., Bastone, A., Salvatori, G., Mantovani, A., Siracusa, G., and Salustri, A. (2007) PTX3 interacts with inter-α-trypsin inhibitor: Implications for hyaluronan organization and cumulus oophorus expansion. *J. Biol. Chem.*

282, 30161–30170
34. Ma, Y. J., Doni, A., Hummelshøj, T., Honoré, C., Bastone, A., Mantovani, A., Thielens, N. M., and Garred, P. (2009) Synergy between ficolin-2 and pentraxin 3 boosts innate immune recognition and complement deposition. *J. Biol. Chem.* **284,** 28263–28275
35. Salustri, A., Garlanda, C., Hirsch, E., De Acetis, M., Maccagno, A., Bottazzi, B., Doni, A., Bastone, A., Mantovani, G., Beck Peccoz, P., Salvatori, G., Mahoney, D. J., Day, A. J., Siracusa, G., Romani, L., and Mantovani, A. (2004) PTX3 plays a key role in the organization of the cumulus oophorus extracellular matrix and in in vivo fertilization. *Development* **131,** 1577–1586
36. Inforzato, A., Peri, G., Doni, A., Garlanda, C., Mantovani, A., Bastone, A., Carpentieri, A., Amoresano, A., Pucci, P., Roos, A., Daha, M. R., Vincenti, S., Gallo, G., Carminati, P., De Santis, R., and Salvatori, G. (2006) Structure and function of the long pentraxin PTX3 glycosidic moiety: Fine-tuning of the interaction with C1q and complement activation. *Biochemistry* **45,** 11540–11551
37. Pereira, H. A., Shafer, W. M., Pohl, J., Martin, L. E., and Spitznagel, J. K. (1990) CAP37, a human neutrophil-derived chemotactic factor with monocyte specific activity. *J. Clin. Invest.* **85,** 1468–1476
38. Soehnlein, O., and Lindbom, L. (2009) Neutrophil-derived azurocidin alarms the immune system. *J. Leukocyte Biol.* **85,** 344–351
39. Hirsch, J. G. (1958) Bactericidal action of histone. *J. Exp. Med.* **108,** 925–944
40. Klebanoff, S. J. (2005) Myeloperoxidase: Friend and foe. *J. Leukocyte Biol.* **77,** 598–625
41. Kothari, N., Keshari, R. S., Bogra, J., Kohli, M., Abbas, H., Malik, A., Dikshit, M., and Barthwal, M. K. (2010) Increased myeloperoxidase enzyme activity in plasma is an indicator of inflammation and onset of sepsis. *J. Crit. Care* **26,** 435, e1–7
42. Linder, A., Christensson, B., Herwald, H., Björck, L., and Akesson, P. (2009) Heparin-binding protein: An early marker of circulatory failure in sepsis. *Clin. Infect. Dis.* **49,** 1044–1050
43. Berkestedt, I., Herwald, H., Ljunggren, L., Nelson, A., and Bodelsson, M. (2010) Elevated plasma levels of antimicrobial polypeptides in patients with severe sepsis. *J. Innate Immun.* **2,** 478–482